ISSN 0005-1179 (print), ISSN 1608-3032 (online), Automation and Remote Control, 2024, Vol. 85, No. 12, pp. 1149–1167.

STOCHASTIC SYSTEMS

AUV Positioning and Motion Parameter Identification Based on Observations with Random Delays

A. V. Bosov

Federal Research Center "Computer Science and Control," Russian Academy of Sciences, Moscow, Russia
e-mail: ABosov@frccsc.ru

Received June 20, 2024
Revised September 10, 2024
Accepted September 20, 2024

Abstract—A stochastic observation system model with random time delays between an arriving observation and the factual state of a moving object is adapted to identify its motion parameters. Equations for optimal Bayesian identification are given. A conditionally minimax nonlinear filter (CMNF) is applied to solve the problem in practice. The design procedure of the CMNF, including the choice of the filter structure, is discussed in detail on an example of autonomous underwater vehicle (AUV) positioning based on observations of stationary acoustic beacons. A computational experiment is carried out on a model close to practical needs using three variants of the filter, namely, the typical approximation of the updating process, the method of linear pseudomeasurements, and the geometric interpretation of angular measurements.

Keywords: nonlinear stochastic observation system, parameter identification, observations with random delays, conditionally minimax nonlinear filter, positioning, acoustic sensors, linear pseudomeasurements

DOI: 10.31857/S0005117924120029

1. INTRODUCTION

The theory of stochastic filtering provides methods and algorithms for solving various applied problems of estimation and control of moving objects [1]. In turn, applications may be sources of new formulations, models, and criteria, stimulating the improvement and development of the theory. One example is the applied field of autonomous underwater vehicles (AUVs) [2]. The peculiarities of the aquatic environment affect not only the nature and goals of the motion but also measuring means. For instance, different measuring means can be used for AUV positioning [3]; however, they all involve common physical laws. They are acoustic sensors, i.e., their operation depends on many factors, from water temperature to salinity and pressure [4]. As a result, data on the state of the observed AUV arrive with a random delay. This factor is not considered in the analogous problem of aircraft navigation because the high velocity of radio wave propagation allows one to neglect it. Indeed, the models of radar surveillance systems assume that data on the current position of an aircraft are acquired at the current time instant. However, the velocity of acoustic wave propagation is not so high, so the delay may be quite large and cannot be neglected. The stochastic dynamic observation system model with the delay factor of the acoustic signal was proposed in [5] and supplemented in [6]. Formally, this model can be reduced to the unified representation of a nonlinear stochastic observation system; as a result, it becomes possible to write optimal Bayesian filtering relations for it [7] and apply well-known heuristic filtering methods, including the extended Kalman filter [8], particle filters [9], and different modifications of sigma-point filters [10]. Meanwhile, both the optimal filter and any heuristic estimates cannot be used in practice even on model examples since the factor of a random time delay between an arriving

observation and the factual state of a moving object is compensated via augmenting the state vector by a value proportional to the delay time and the measurement frequency. Under near-realistic conditions, one obtains a huge dimension, with no prospect of handling it. The only effective tool to cope with delays is given by Pugachev's method of conditionally optimal filtering [11, 12] and its development, Pankov's conditionally minimax nonlinear filter (CMNF) [13]. This conclusion was confirmed by calculations [5, 6]. Continuing to investigate the CMNF in the time-delay model, this paper focuses on two issues. First, the quality of conditionally optimal filtering is largely determined by a reasonable choice of the filter structure. Universal recommendations [14] can strongly lose to solutions considering the problem's specifics. This fact was demonstrated, in particular, in [5, 6], where the filter was successfully designed based on a simple geometric interpretation of measurements. The same idea is employed below not for a simplified model example but for that with real application content, and the results seem also good. However, such a variant of measurements (with direct position determination by solving a geometric problem) still has limited capabilities, and a more universal approach is needed here. Such an approach utilizes the linear pseudomeasurement method proposed in [15] and successfully developed in [16]. The corresponding results are presented in Section 4, including a stochastic observation system model describing the AUV positioning process using the angular measurements of two acoustic beacons and variants for choosing the CMNF structure that agree with the physical meaning of the problem. This example shows how angular measurements can improve the positioning accuracy considering the time delay of observations caused by the aquatic environment. The second issue concerns the traditional assumption for stochastic observation systems that the state model of a moving object is known. In practice, this assumption is incompletely valid, and the models are used with some errors. It is possible to compensate for the influence of such errors by including their model in the state equations. Many problems and methods of this kind have been created in the theory of robust estimation [17]. Another alternative is to describe the model inaccuracies by parameters, estimate them, and use the estimates together with the solution of the basic filtering problem. The corresponding methods belong to the theory of identification [18], regardless of whether this is possible and whether these parameters are estimated in advance or simultaneously with the estimation of the current position of the object. It seems rather natural to combine filtering and identification problems by forming an observation system model within the Bayesian approach. This variant of the CMNF with application to the AUV positioning problem is implemented below. Section 2 describes the formal model of a stochastic system with random time delays of measurements and the unknown parameters of the state model. In Section 3, we adapt the optimal filtering equations [5, 6] and the equations for the CMNF parameters used for positioning in the numerical experiment to the case of Bayesian parameter identification. In parallel with positioning, we identify the unknown motion parameters determining the average constant velocity of the AUV. Hence, it becomes possible to estimate the influence of the identification results of the motion model on the quality of solving the (main) positioning problem and, when using only angular position measurements, assess the fundamental possibility of estimating the motion velocity without its direct measurement, e.g., by Doppler sensors.

2. MOTION PARAMETER IDENTIFICATION MODEL BASED ON OBSERVATIONS WITH RANDOM DELAYS

The AUV motion and the set of measurements are described by a discrete stochastic dynamic system with unknown parameters. By assumption, the maximum possible time delay of arriving observations, T, is a priori given. Since the sound velocity in water can be supposed to be known, this assumption is reduced to estimating the maximum distance between the meters and the AUV, which should not be difficult. Denoting by $t = 0$ the initial positioning time instant, for the discrete time variable t we have $t = -T, -T+1, \ldots, 0,\ 1, \ldots$.

The AUV position, defined by a vector $x_t = (x_{1t}, \ldots, x_{p_t})' \in \mathbb{R}^p$ (e.g., the coordinates $(x(t), y(t), z(t))'$ and velocities $(v_x(t), v_y(t), v_z(t))'$ in an inertial reference frame linked to the Earth), and a random vector $\mu = (\mu_1, \ldots, \mu_r)' \in \mathbb{R}^r$ of unknown motion model parameters form the state vector $(x_t', \mu')' \in \mathbb{R}^{p+r}$ of the dynamic system. Throughout this paper, "$'$" indicates the transpose of an appropriate vector or matrix. Let the distribution of μ be given.

The observation vector $y_t = (y_{1t}, \ldots, y_{q_t})' \in \mathbb{R}^q$ consists of measurements containing additive errors and time delays. Each observation element y_{it} has a particular shift described by a discrete random variable τ_{it} with values from the set $\{0, 1, \ldots, T\}$. The values τ_{it} are combined into the vector $\tau_t = (\tau_{1t}, \ldots, \tau_{q_t})' \in \mathbb{R}^q$, which is a function of x_t. Exactly, each observation element y_{it} is a measurement performed for the position $x_{t-\tau_{it}}$. Thus, the observation system has the form

$$\begin{gathered} x_t = \varphi_t(x_{t-1}, \mu) + w_t, \quad x_{-T-1} = \eta, \\ y_{it} = \psi_{it}\left(x_{t-\tau_{it}}\right) + v_{it}, \quad i = 1, \ldots, q, \\ \tau_t = \theta_t(x_t), \end{gathered} \tag{1}$$

where $w_t = (w_{1t}, \ldots, w_{p_t})' \in \mathbb{R}^p$ is a vector discrete white noise that models disturbances, $\eta \in \mathbb{R}^p$ are initial conditions, and $v_t = (v_{1t}, \ldots, v_{q_t})' \in \mathbb{R}^q$ is a vector discrete white noise that models measurement errors. The vectors η, μ, w_t, and v_t are independent in the aggregate, and the known functions φ_t, ψ_t, and θ_t satisfy sufficient conditions for the existence of filtering, Bayesian, and conditionally minimax estimates. These are typical conditions ensuring the existence of the second moment for the state and observation vectors, e.g., the linear growth of the system functions at infinity and the presence of the second moments for the disturbances and observation errors; see Theorems 1 and 2 in [5].

In model (1), we can introduce a compound state vector including both the AUV coordinates and the unknown random parameters of the motion model: $(x_t', \mu_t')'$. Then the observation system model takes the form

$$\begin{gathered} x_t = \varphi_t(x_{t-1}, \mu_{t-1}) + w_t, \quad x_{-T-1} = \eta, \\ \mu_t = \mu_{t-1}, \quad \mu_{-T-1} = \mu, \\ y_t = \psi_t(x_{t-\tau_t}) + v_t, \quad \tau_t = \theta_t(x_t). \end{gathered} \tag{2}$$

To make model (2) correct and usable as a formal representation of (1), we clarify that the notation $x_{t-\tau_t}$ is the vector $\left(x'_{1_{t-\tau_{1t}}}, \ldots, x'_{p_{t-\tau_{q_t}}}\right)'$ of the AUV positions corresponding to the time delay of each measurement included in the observation vector y_t.

In accordance with the Bayesian interpretation of the identification problem, it is required to specify a probability density for the initial condition vector $(\eta', \mu')'$. This density can be written as

$$f_0(X_{-T-1}, M) = f_\eta(X_{-T-1})\, f_\mu(M), \tag{3}$$

where $X_{-T-1} \in \mathbb{R}^p$ and $M \in \mathbb{R}^r$ are the arguments of the probability densities corresponding to the random vectors η and μ, which have been supposed to be independent above.

Now, for the observation system (2), we can pose a filtering problem: it is required to estimate the state $(x_t', \mu_t')'$ based on the observations $y^t = (y_0', \ldots, y_t')'$. Solving the filtering problem for the compound state vector yields a solution for both the positioning problem (estimation of the current position x_t) and the parameter identification problem (estimation of the vector μ).

3. FILTERING ALGORITHMS

Note that in the problem under consideration, the optimal Bayesian filter can be described by recurrence relations for the posterior probability density. Similar relations are well known for

conventional discrete observation systems (without delays) [19]; they were generalized to the case of time-delayed systems in [7]. Clearly, the same result holds in the problem to be solved. The filter is written for the augmented position vector $\mathbf{x}_t = \left(x'_{t-T}, \ldots, x'_{t-1}, x'_t\right)'$ because all possible time delays need to be considered. For a less cumbersome notation, we simplify the time-delay model by assuming the scalar value $\tau_t \in \mathbb{R}^1$ instead of the vector $\tau_t \in \mathbb{R}^q$. This happens in the special case $\tau_{1t} = \ldots = \tau_{q_t}$. In other words, all observers are located at approximately the same distance from the AUV, e.g., when there is only one measuring complex.

It is possible to write the posterior probability density $\rho_t = \rho_t\left(\mathbf{X}_t, M|Y^t\right)$ of the vector $(\mathbf{x}'_t, \mu')'$ with respect to the vector of all observations, y^t, and the filtering estimates of the position and parameters, x_t^* and μ_t^*. For this purpose, for the sake of convenience, we denote by $\mathbf{X}_t = \left(X'_{t-T}, \ldots, X'_{t-1}, X'_t\right)'$, $M = (M_1, \ldots, M_r)'$, and $Y^t = (Y'_0, \ldots, Y'_t)'$ the arguments of the posterior density; they correspond to the vectors $\mathbf{x}_t$, μ, and y^t, respectively. In addition, we employ the unnormalized posterior density $\widehat{\rho}_t = \widehat{\rho}_t\left(\mathbf{X}_t, M|Y^t\right)$, so

$$\rho_t\left(\mathbf{X}_t, M\middle|Y^t\right) = \frac{\widehat{\rho}_t\left(\mathbf{X}_t, M|Y^t\right)}{\int \widehat{\rho}_t\left(\mathbf{X}_t, M|Y^t\right) d\mathbf{X}_t dM}.$$

Then we have [7]

$$\begin{gathered}\widehat{\rho}_t\left(\mathbf{X}_t, M\middle|Y^t\right) = f_{w_t}\left(X_t - \varphi_t\left(X_{t-1}, M\right)\right) \\ \times \sum_{i=0}^{T} I\left(\theta_t\left(X_t\right) = i\right) f_{v_t}\left(Y_t - \psi_t\left(X_{t-i}\right)\right) \int \rho_{t-1} dX_{t-T-1},\end{gathered} \tag{4}$$

where $f_{w_t}(\cdot)$ is the probability density of the disturbances w_t and $f_{v_t}(\cdot)$ is the probability density of the observation errors. Equation (4) is solved with the initial condition

$$\begin{gathered}\rho_{-1}\left(\mathbf{X}_{-1}, M\middle|Y^{-1}\right) = \rho_{-1}\left(\mathbf{X}_{-1}, M\right) = \rho_{-1}\left(X_{-T-1}, \ldots, X_{-1}, M\right) \\ = f_0\left(X_{-T-1}, M\right) f_{w_{-T}}\left(X_{-T} - \varphi_{-T}\left(X_{-T-1}, M\right)\right) \ldots f_{w_{-1}}\left(X_{-1} - \varphi_{-1}\left(X_{-2}, M\right)\right).\end{gathered}$$

The Bayesian estimates x_t^* and μ_t^* are obtained by integration:

$$\left((\mathbf{x}_t^*)', (\mu_t^*)'\right)' = \int \left(\mathbf{X}'_t, M'\right)' \rho_t\left(\mathbf{X}_t, M\middle|Y^t\right) d\mathbf{X}_t dM, \quad \mathbf{x}_t^* = \left(\ldots, (x_t^*)'\right)'.$$

According to the last equality, the current position estimate x_t^* enters as the last subvector in $\mathbf{x}_t^*$; also, the estimates of the past AUV positions have to be computed, although they are unnecessary.

The main conclusion from these considerations is that, despite the fundamental possibility of obtaining the optimal filtering and Bayesian identification estimates, we cannot reckon on their practical use. In the AUV positioning model described below, implementing calculations by formula (4) would have to deal with the dimensions $p = 3$, $r = 3$, $q = 4$, and $T = 15$, which gives the augmented vector $\mathbf{X}_t$ of dimension 45. For such dimensions, it seems at least rash to expect success in computing integrals with good accuracy under the real-time arrival of observations y_t.

Thus, a different approach to filtering is needed here to obtain a practically implementable estimate, albeit not optimal, but with good accuracy. Among many known approaches to suboptimal filtering, the concept of conditionally optimal filtering [11, 12] allows considering the specifics of the model of random observation delays without making cardinal changes. The possibility to flexibly change the filter structure based on the peculiarities of a particular observation system, originally envisaged by this concept, will make it possible to consider both the time delays and

the physical laws determining the AUV motion and the operation of the sensors. The minimax explanation of the properties of this filter and the idea to calculate its parameters approximately by simulation [13] give grounds for obtaining good-quality estimates both in the positioning problem and in the motion parameter identification problem as the implementability of the corresponding algorithms with reasonable computational cost is its inherent property.

Following [13] and using the notations of this paper, we write the CMNF estimate $\left((\widehat{x}_t)', (\widehat{\mu}_t)'\right)'$ of the position x_t and the random motion model parameters μ based on the observations y^t in the prediction-correction form

$$\widehat{x}_t = \widetilde{x}_t + \Delta\widehat{x}_t, \quad \widehat{\mu}_t = \widehat{\mu}_{t-1} + \Delta\widehat{\mu}_t.$$

The position prediction $\widetilde{x}_t$ is calculated using the basic prediction function $\xi_t(X, M)$; the correction, using the basic correction function $\zeta_t(X, Y)$, $X \in \mathbb{R}^p$, $M \in \mathbb{R}^r$, $Y \in \mathbb{R}^q$. The prediction $\widetilde{x}_t$ is calculated as a function of $\xi_t = \xi_t(\widehat{x}_{t-1}, \widehat{\mu}_{t-1})$ whereas the correction $(\Delta\widehat{x}_t', \Delta\widehat{\mu}_t')'$ as a function of $\zeta_t = \zeta_t(\widetilde{x}_t, y_t)$. Note that the correction does not involve the parameter estimate $\widehat{\mu}_{t-1}$ (no argument M), which is explained by the absence of the parameters in the observation function.

The functions implementing $\widetilde{x}_t$ and $\Delta\widehat{x}_t$ are chosen linear so that

$$\begin{gathered} \widetilde{x}_t = F_t\xi_t(\widehat{x}_{t-1}, \widehat{\mu}_{t-1}) + f_t, \\ \begin{pmatrix} \widehat{x}_t \\ \widehat{\mu}_t \end{pmatrix} = \begin{pmatrix} \widetilde{x}_t \\ \widehat{\mu}_{t-1} \end{pmatrix} + H_t\zeta_t(\widetilde{x}_t, y_t) + h_t, \end{gathered} \tag{5}$$

where

$$\begin{gathered} F_t = \operatorname{cov}(x_t, \xi_t)\operatorname{cov}^+(\xi_t, \xi_t), \ f_t = \mathrm{E}\{x_t\} - F_t\mathrm{E}\{\xi_t\}, \\ H_t = \operatorname{cov}\left(\begin{pmatrix} x_t \\ \mu \end{pmatrix} - \begin{pmatrix} \widetilde{x}_t \\ \widehat{\mu}_{t-1} \end{pmatrix}, \zeta_t\right)\operatorname{cov}^+(\zeta_t, \zeta_t), \ h_t = -H_t\mathrm{E}\{\zeta_t\}. \end{gathered} \tag{6}$$

Formulas (6) have the following notations: $\mathrm{E}\{x\}$ is the expectation of the random vector x, $\operatorname{cov}(x, y)$ is the covariance of x and y, and "+" is the Moore–Penrose pseudoinverse [20]. In addition, the position prediction $\widetilde{x}_t$ and the estimates $\widehat{x}_t$ and $\widehat{\mu}_t$ are unbiased with the estimation error covariances

$$\begin{aligned} \widetilde{K}_t &= \operatorname{cov}(x_t - \widetilde{x}_t, x_t - \widetilde{x}_t) = \operatorname{cov}(x_t, x_t) - F_t\operatorname{cov}(\xi_t, x_t), \\ \widehat{K}^x_t &= \operatorname{cov}(x_t - \widehat{x}_t, x_t - \widehat{x}_t) = \widetilde{K}_t - \Delta\widehat{K}^x_t, \quad \widetilde{K}_0 = \operatorname{cov}(\eta, \eta), \\ \widehat{K}^\mu_t &= \operatorname{cov}(\mu - \widehat{\mu}_t, \mu - \widehat{\mu}_t) = \widehat{K}^\mu_{t-1} - \Delta\widehat{K}^\mu_t, \quad \widetilde{K}_0 = \operatorname{cov}(\mu, \mu), \end{aligned} \tag{7}$$

where the matrices $\Delta\widehat{K}^x_t$ and $\Delta\widehat{K}^\mu_t$ are the upper and lower diagonal blocks of the matrix $H_t\operatorname{cov}\left(\zeta_t, \begin{pmatrix} x_t \\ \mu \end{pmatrix} - \begin{pmatrix} \widetilde{x}_t \\ \widehat{\mu}_{t-1} \end{pmatrix}\right) = \begin{pmatrix} \Delta\widehat{K}^x_t & \dots \\ \dots & \Delta\widehat{K}^\mu_t \end{pmatrix}$.

The linear transformations (5) of the basic prediction ξ_t and correction ζ_t have minimax justification as the best estimates on the classes of all probability distributions with known mean and covariance [13]. In practical calculations, Monte Carlo estimates of the filter coefficients F_t, f_t, H_t, and h_t are used instead of their analytical values. In other words, $\mathrm{E}\{x\}$ in (6) is replaced by $\overline{\mathrm{E}}\{x\} = \frac{1}{N}\sum_{i=1}^N x_i$, where $\{x_i\}_{i=1}^N$ are the sample values of x simulated on a computer. Finally, sufficient conditions for the existence of the estimate (5) with respect to model (2) were formulated in [5, 6].

Thus, to solve the AUV positioning problem, it is required to specify motion and observation conditions and design the CMNF by selecting the basic prediction ξ_t and correction ζ_t.

4. AUV POSITIONING USING STATIONARY ACOUSTIC BEACONS

4.1. Motion Model

As has already been mentioned, the movement of an object in a water environment is the target (and currently single) application of the considered model of the system with random time delays of observations. Water acts as a natural source of delays in measurements made by various acoustic sensors. Different problems can be formulated using such measurements, including target goal-setting and intelligent target tracking, vehicle position estimation and prediction, motion model identification, individual and group movement planning, inertial navigation and visual positioning, and others. To demonstrate the flexibility and efficiency of the CMNF, we select the positioning problem of an AUV interacting with two stationary acoustic beacons. The observation model and possible approaches to solving the estimation problem in this formulation were discussed in detail in [21–23]. Here, this model is supplemented by introducing random time delays for the measurements of each beacon and inaccurate a priori information on the motion parameters, namely, the average velocity vector of the AUV. Thus, it is possible to analyze the standard application of the CMNF for solving the state filtering problem (determination of the AUV position) as well as positioning together with parameter identification.

The AUV motion model assumes that on average the vehicle moves at a constant velocity, while the real velocity is affected by uncontrolled random factors. Their influence leads to independent deviations of the velocity, which remains constant on sampling intervals (between successive measurements) and changes at each next time instant. The same in-plane motion was used in [5] but under the assumption of known motion parameters. Here, we will identify them.

The AUV motion is described in the Cartesian reference frame $Oxyz$; its choice will be discussed below. The typical notations $x(t)$, $y(t)$, and $z(t)$ are employed for the motion trajectory coordinates; they are measured in kilometers (km). Note the distinction between these notations and x_t, y_t used above for the observation system in the general model (1). AUV positioning starts at the time instant $t = 0$ and is performed at discrete time instants with steps δ: $\delta, 2\delta, \ldots, t\delta, \ldots$. The AUV motion starts at the time instant $-T\delta$, i.e., $t = -T$, so a measurement with any permissible delay $\tau_{0i} \leqslant T$ can be realized at the time instant $t = 0$; therefore, the AUV initial position is given by the vector $(x(-T-1), y(-T-1),\ x(-T-1))'$. In the calculations carried out, this vector is supposed to obey the Gaussian distribution with the mean $(-1, -1, 1)'$ and the covariance diag $\{0.1^2; 0.1^2; 0.1^2\}$. By assumption, the AUV moves at an unknown constant velocity $(v_x, v_y, v_z)'$, which is affected by uncontrolled factors. The absence of accurate velocity information is modeled by making the vector $(v_x, v_y, v_z)'$ Gaussian with the mean $\mathrm{E}\{v_x\} = -25$ km/h, $\mathrm{E}\{v_y\} = -12.5$ km/h, $\mathrm{E}\{v_z\} = -1$ km/h and the covariance diag $\{5^2, 5^2, 1\}$. Thus, each trajectory has a particular "target" motion (direction and velocity) and, along with positioning (estimation of the position $(x(t), y(t), z(t))'$), it is required to identify the parameters of this motion given by the realization of the vector $(v_x, v_y, v_z)'$.

The uncontrolled random factors affecting the velocity of motion are modeled by additive disturbances $w_x(t)$, $w_y(t)$, and $w_z(t)$; by assumption, the vector $(w_x(t), w_y(t), w_z(t))'$ obeys the Gaussian distribution with the mean $(0,\ 0,\ 0)'$ and the covariance diag $\{25^2, 25^2, 25^2, 25^2\}$. Thus, we have the state vector $(x_t', \mu')' = (x(t), y(t), z(t), v_x, v_y, v_z) \in \mathbb{R}^{3+3}$ and the following dynamics:

$$\begin{cases} x(t) = x(t-1) + \delta(v_x + w_x(t)), \\ y(t) = y(t-1) + \delta(v_y + w_y(t)), \\ z(t) = z(t-1) + \delta(v_z + w_z(t)), \\ t = -T, -T+1, \ldots, 0, 1, \ldots. \end{cases} \tag{8}$$

For the other calculation parameters, as in [5], we set a sampling step of $\delta = 0.0001$ hours (h) for observations (i.e., about three measurements per second (s); positioning is performed for 1000 sam-

pling steps, $t = -T, \ldots, 1000$, (i.e., 6 minutes (min) of motion). During this time, the AUV traverses an average distance of about 2.5–3 km, with the maximum range to the farther of the two beacons being 8 km. Accordingly, the maximum time delay is supposed to be $T = 15$, constituting 0.0015 h or 5.4 s. This assumption is based on the sound velocity in water $v_s = 5400$ km/h (1500 m/s).

4.2. Measuring Complex Model

Observers are two stationary acoustic beacons (passive acoustic devices for estimating the direction of arrival (DOA) [24]) installed in advance. Let the first ($\mathcal{F}$, $first$) and second ($\mathcal{S}$, *second*) beacons have the coordinates $(X_\mathcal{F},\ Y_\mathcal{F}, Z_\mathcal{F})$ and $(X_\mathcal{S},\ Y_\mathcal{S}, Z_\mathcal{S})$, respectively. Following the model proposed in [22], observations of the positioned AUV with the unknown coordinates $(X,\ Y, Z)$ are the directions to each of the beacons, which yield two angles

$$\begin{cases} \tan\varphi_\mathcal{F} = \dfrac{Y_\mathcal{F} - Y}{X_\mathcal{F} - X}, \quad \tan\varphi_\mathcal{S} = \dfrac{Y_\mathcal{S} - Y}{X_\mathcal{S} - X}, \\ \tan\lambda_\mathcal{F} = \dfrac{Z_\mathcal{F} - Z}{|X_\mathcal{F} - X|}\cos\varphi_\mathcal{F}, \quad \tan\lambda_\mathcal{S} = \dfrac{Z_\mathcal{S} - Z}{|X_\mathcal{S} - X|}\cos\varphi_\mathcal{S}. \end{cases} \tag{9}$$

Figure 1 shows the geometric interpretation of the measured angles, particularly how the angles $\varphi_\mathcal{F}$, $\varphi_\mathcal{S}$, $\lambda_\mathcal{F}$, and $\lambda_\mathcal{S}$ can be counted to determine the mutual position of the beacon and the positioned AUV in order to correctly find the vehicle's position based on the available tangent measurements and consider the possible crossing of the lines $X_\mathcal{F} - X = 0$ and $X_\mathcal{S} - X = 0$ when some measurements cannot be used. In this figure, positions 1-2-3-4 of the AUV (X_1, Y_1, Z_1) and the beacon $(X_\mathcal{M}, Y_\mathcal{M}, Z_\mathcal{M})$ correspond to possible combinations of the coordinates $X_1 < X_\mathcal{M}$, $X_1 > X_\mathcal{M}$, $Y_1 < Y_\mathcal{M}$, $Y_1 > Y_\mathcal{M}$, and the angles φ and λ are counted so that relation (9) holds in all variants.

In the experiment described below, assuming the cooperative scenario (the beacons and the AUV act jointly to fulfill their common task), it is possible to simplify the relations slightly by

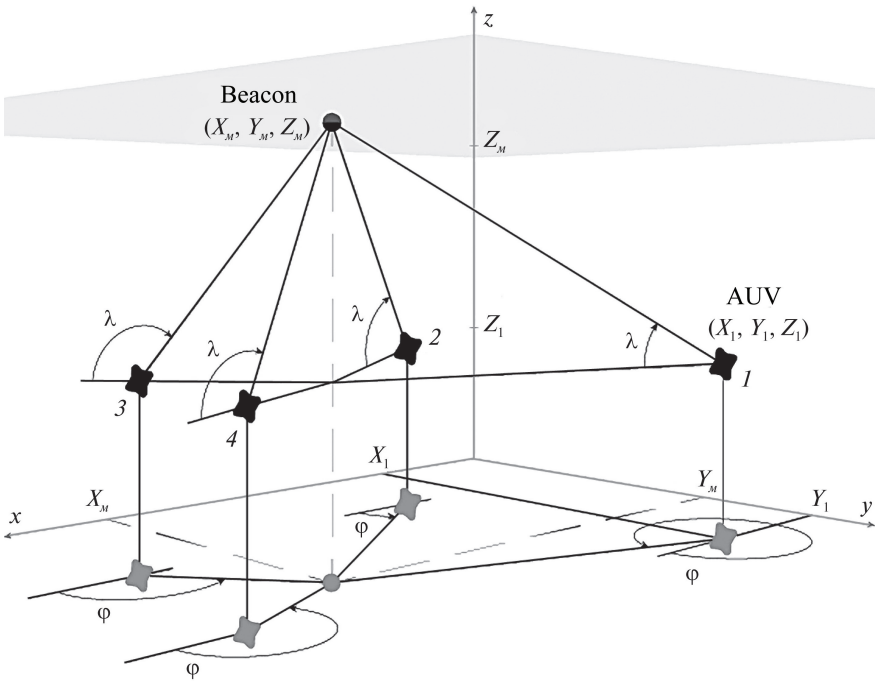

Fig. 1. Possible mutual arrangement of the AUV and beacons.

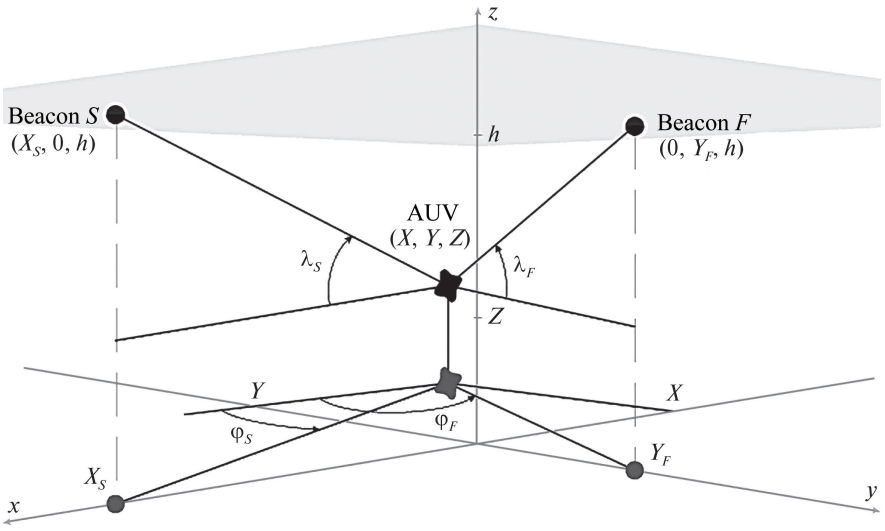

Fig. 2. Mutual arrangement of the AUV and two beacons in the experiment.

choosing a reference frame so that $(X_{\mathcal{F}}, Y_{\mathcal{F}}, Z_{\mathcal{F}}) = (0, Y_{\mathcal{F}}, h)$ and $(X_{\mathcal{S}}, Y_{\mathcal{S}}, Z_{\mathcal{S}}) = (X_{\mathcal{S}}, 0, h)$, where h is the depth at the location of the beacons (Fig. 2). Also, we may assume that $X_{\mathcal{F}} > 0$, $Y_{\mathcal{F}} > 0$ and the origin is located so that $X < 0$, $Y < 0$ throughout the entire motion time. Then all the measured angles $\varphi_{\mathcal{F}}$, $\varphi_{\mathcal{S}}$, $\lambda_{\mathcal{F}}$, and $\lambda_{\mathcal{S}}$ will vary in the range $(0, \frac{\pi}{2})$, so $\cos\varphi_{\mathcal{F}} = \frac{1}{(1+\tan^2\varphi_{\mathcal{F}})^{1/2}}$ and $\cos\varphi_{\mathcal{S}} = \frac{1}{(1+\tan^2\varphi_{\mathcal{S}})^{1/2}}$. Thus, we arrive at the following relations of the measurements instead of (9):

$$\begin{cases} \tan\varphi_{\mathcal{F}} = \dfrac{Y - Y_{\mathcal{F}}}{X}, \quad \tan\varphi_{\mathcal{S}} = \dfrac{Y}{X - X_{\mathcal{S}}}, \\ \tan\lambda_{\mathcal{F}} = \dfrac{Z-h}{X}\cos\varphi_{\mathcal{F}}, \quad \tan\lambda_{\mathcal{S}} = \dfrac{Z-h}{X - X_{\mathcal{S}}}\cos\varphi_{\mathcal{S}}. \end{cases} \tag{10}$$

In the calculations carried out, the coordinates of the beacons are given by $Y_{\mathcal{F}} = 1$ km and $X_{\mathcal{S}} = 2$ km, the depth is $h = 2$ km. Accordingly, with the expected initial position $(-1, -1, 1)'$ and average velocity $(-25; -12.5; -1)'$ of the AUV chosen above, the vehicle will move away from both beacons and maintain negative coordinates $x(t), y(t)$ and positive coordinates $z(t)$ on average during 6 min of its positioning. Increasing the distance to the observers means increasing the values taken by the time delay τ_t.

Therefore, it remains to consider the measurement errors in (10). According to model (1), they are additive, so the factual model of the measuring complex without time delays in arriving observations has the form

$$\begin{cases} y_{1t} = \dfrac{y(t) - Y_{\mathcal{F}}}{x(t)} + v_1(t), \quad y_{2t} = \dfrac{z(t)-h}{x(t)}\dfrac{1}{(1+\tan^2\varphi_{\mathcal{F}}(t))^{1/2}} + v_2(t), \\ y_{3t} = \dfrac{y(t)}{x(t) - X_{\mathcal{S}}} + v_3(t), \quad y_{4t} = \dfrac{z(t)-h}{x(t)-X_{\mathcal{S}}}\dfrac{1}{(1+\tan^2\varphi_{\mathcal{S}}(t))^{1/2}} + v_4(t), \\ \tan\varphi_{\mathcal{F}}(t) = \dfrac{y(t) - Y_{\mathcal{F}}}{x(t)}, \quad \tan\varphi_{\mathcal{S}}(t) = \dfrac{y(t)}{x(t) - X_{\mathcal{S}}}, \end{cases} \tag{11}$$

where $y_t = (y_{1t}, y_{2t}, y_{3t}, y_{4t})'$ is the vector of the measured angular directions $\tan\varphi_{\mathcal{F}}$, $\tan\lambda_{\mathcal{F}}$, $\tan\varphi_{\mathcal{S}}$, and $\tan\lambda_{\mathcal{S}}$; the AUV coordinates $x(t)$, $y(t)$, and $z(t)$ are given by model (8), and the vector

$(v_1(t), v_2(t), v_3(t), v_4(t))'$ of the additive measurement errors obeys the Gaussian distribution with the mean $(0,0,0,0)'$ and the covariance diag $\{(0,01)^2, (0,01)^2, (0,01)^2, (0,01)^2\}$. In the described experiment, the accuracy characteristics of the simulated acoustic sensors are chosen so that differences in the estimates can be visualized while maintaining an acceptable quality of all algorithms. The relative accuracy of real devices was discussed in [25].

To consider the observation delays τ_t in (11), we define two random functions $\tau_{\mathcal{F}}(t)$ and $\tau_{\mathcal{S}}(t)$, which will model the acoustic signal delay in time cycles, i.e., in the sampling steps δ, under the constant sound velocity v_s (see the assumption above). Note that for the problem under study, this simplified assumption is sufficient. In practice, it can be replaced without much difficulty by a more precise relation, e.g., the value obtained using the algorithm [26] or other simpler approximations [27]. Knowing the AUV current position $(x(t), y(t), z(t))'$, we calculate the ranges to the beacons located at the points $(0, Y_{\mathcal{F}}, h)$ and $(X_{\mathcal{S}}, 0, h)$, and the delays $\tau_{\mathcal{F}}(t)$ and $\tau_{\mathcal{S}}(t) \in \{0, 1, \ldots, T\}$ in time units of the motion model (8):

$$\begin{cases} \tau_{\mathcal{F}}(t) = \min\left\{T, \left[\dfrac{\sqrt{(x(t))^2 + (y(t) - Y_{\mathcal{F}})^2 + (z(t) - h)^2}}{(\delta v_s)}\right]\right\}, \\ \tau_{\mathcal{S}}(t) = \min\left\{T, \left[\dfrac{\sqrt{(x(t) - X_{\mathcal{S}})^2 + (y(t))^2 + (z(t) - h)^2}}{(\delta v_s)}\right]\right\}. \end{cases} \tag{12}$$

In (12) we use the notation $[x]$ for the floor function of x and the minimum to make the delays formally correspond to the model (1) and not exceed the given threshold T. In the calculations, $T = 15$ (large enough) and this minimum constraint was never activated on the simulated trajectories.

Thus, the observation model takes the final form

$$\begin{cases} y_{1t} = \dfrac{x_{2t-\tau_{\mathcal{F}}(t)} - Y_{\mathcal{F}}}{x_{1t-\tau_{\mathcal{F}}(t)}} + v_1(t), \ y_{2t} = \dfrac{x_{3t-\tau_{\mathcal{F}}(t)} - h}{x_{1t-\tau_{\mathcal{F}}(t)}} \dfrac{1}{(1 + \tan^2 \varphi_{\mathcal{F}}(t - \tau_{\mathcal{F}}(t)))^{1/2}} + v_2(t), \\ y_{3t} = \dfrac{x_{2t-\tau_{\mathcal{S}}(t)}}{x_{1t-\tau_{\mathcal{S}}(t)} - X_{\mathcal{S}}} + v_3(t), \ y_{4t} = \dfrac{x_{3t-\tau_{\mathcal{S}}(t)} - h}{x_{1t-\tau_{\mathcal{S}}(t)}} \dfrac{1}{(1 + \tan^2 \varphi_{\mathcal{S}}(t - \tau_{\mathcal{S}}(t)))^{1/2}} + v_4(t), \\ \tan \varphi_{\mathcal{F}}(t) = \dfrac{x_{2t} - Y_{\mathcal{F}}}{x_{1t}}, \quad \tan \varphi_{\mathcal{S}}(t) = \dfrac{x_{2t}}{x_{1t} - X_{\mathcal{S}}}. \end{cases} \tag{13}$$

To reduce the delay time in (13) to the form of the original model (1), in which $\tau_t \in \mathbb{R}^4$, we have to use (12) and let $\tau_{1t} = \tau_{2t} = \tau_{\mathcal{F}}(t)$ and $\tau_{3t} = \tau_{4t} = \tau_{\mathcal{S}}(t)$.

4.3. CMNF Design

The filter design procedure consists in selecting its structural functions ξ_t, ζ_t and carrying out computer simulation to calculate the coefficients by formulas (6) and determine the accuracy by formulas (7). For simplicity, we will not introduce separate notations for the CMNF estimates corresponding to different variants of the structural functions, all estimates are indicated in the same way: $\widehat{x}_t$, $\widehat{\mu}_t$, like the predictions $\widetilde{x}_t$. The particular structure of the filter is specified by its name (typical, geometric, or pseudomeasurements).

The three filter variants proposed here involve the basic prediction due to system (8), i.e., $\xi_t \in \mathbb{R}^3$, $t = 0, 1, \ldots$, and have the form

$$\xi_{1t} = X_1 + \delta M_1, \quad \xi_{2t} = X_2 + \delta M_2, \quad \xi_{3t} = X_3 + \delta M_3. \tag{14}$$

The motion equations (8) are linear, which does not affect the presence of parameters to be identified, so the basic prediction (14) is used in all CMNF variants and it makes sense to discuss only the correction process.

In the first variant of the filter, called *typical*, the basic correction is given by the observation residual adjusted by the estimate of the observation delay, i.e., $\zeta_t \in \mathbb{R}^4$, $t = 0, 1, \ldots$. It has the form

$$\begin{cases} \zeta_{1t} = Y_1 - \dfrac{X_2 - Y_{\mathcal{F}}}{X_1}, \quad \zeta_{2t} = Y_2 - \dfrac{X_3 - h}{X_1}\dfrac{1}{(1+\tan^2\widetilde{\varphi}_{\mathcal{F}})^{1/2}}, \\ \tan\widetilde{\varphi}_{\mathcal{F}} = \dfrac{X_2 - Y_{\mathcal{F}}}{X_1}, \quad (X_1, X_2, X_3)' = \widetilde{x}_{t-\widehat{\tau}_{\mathcal{F}}(t)}, \\ \zeta_{3t} = Y_3 - \dfrac{X_2}{X_1 - X_{\mathcal{S}}}, \quad \zeta_{4t} = Y_4 - \dfrac{X_3 - h}{X_1}\dfrac{1}{(1+\tan^2\widetilde{\varphi}_{\mathcal{S}})^{1/2}}, \\ \tan\widetilde{\varphi}_{\mathcal{S}} = \dfrac{X_2}{X_1 - X_{\mathcal{S}}}, \quad (X_1, X_2, X_3)' = \widetilde{x}_{t-\widehat{\tau}_{\mathcal{S}}(t)}, \\ \widehat{\tau}_{\mathcal{F}}(t) = \min\left\{T, \left[\dfrac{\sqrt{(X_1)^2 + (X_2 - Y_{\mathcal{F}})^2 + (X_3 - h)^2}}{(\delta v_s)}\right]\right\} \quad (X_1, X_2, X_3)' = \widetilde{x}_t, \\ \widehat{\tau}_{\mathcal{S}}(t) = \min\left\{T, \left[\dfrac{\sqrt{(X_1 - X_{\mathcal{S}})^2 + (X_2)^2 + (X_3 - h)^2}}{(\delta v_s)}\right]\right\} \quad (X_1, X_2, X_3)' = \widetilde{x}_t. \end{cases} \tag{15}$$

Note that to form the residual, the prediction-related argument of the basic correction ζ_t must contain not only the last position prediction $\widetilde{x}_t$ calculated using (5) but also all previous ones $\widetilde{x}_{t-1}, \ldots, \widetilde{x}_{t-T}$ since the time delay estimates $\widehat{\tau}_{\mathcal{F}}(t)$ and $\widehat{\tau}_{\mathcal{S}}(t)$ in (15) may take any value from 0 to T. The prediction shift is needed to determine the residual from the estimate of the state associated with the current observation y_t, i.e., from the delayed state. This state can be estimated by the values $\widehat{\tau}_{\mathcal{F}}(t)$ and $\widehat{\tau}_{\mathcal{S}}(t)$ for the first and second pair of the measured angles, respectively. In this case, the delay estimates can be calculated using the current position prediction $\widetilde{x}_t$ since the AUV velocity is much less than the sound velocity, so the range to the AUV during the "delivery" time of the measurement (and hence this time) will not change significantly.

The second variant of the CMNF correction employs the method of *pseudomeasurements* [15] as follows. Clearly, the relations for the measured angles can be easily transformed from the original geometric relations (10) into linear combinations of the coordinates to be determined:

$$\begin{cases} \dfrac{Y_{\mathcal{F}}}{\tan\varphi_{\mathcal{F}}} = \dfrac{Y}{\tan\varphi_{\mathcal{F}}} - X, \quad h\dfrac{\cos\varphi_{\mathcal{F}}}{\tan\lambda_{\mathcal{F}}} = Z\dfrac{\cos\varphi_{\mathcal{F}}}{\tan\lambda_{\mathcal{F}}} - X, \\ X_{\mathcal{S}}\tan\varphi_{\mathcal{S}} = X\tan\varphi_{\mathcal{S}} - Y, \quad h\cos\varphi_{\mathcal{S}} - X_{\mathcal{S}}\tan\lambda_{\mathcal{S}} = Z\cos\varphi_{\mathcal{S}} - X\tan\lambda_{\mathcal{S}}. \end{cases}$$

Applying similar transformations to (11) yields

$$\begin{cases} \dfrac{Y_{\mathcal{F}}}{y_{1t}} = \dfrac{y(t)}{y_{1t}} - x(t) + \dfrac{x(t)}{y_{1t}}v_1(t), \\ \dfrac{h}{(1+\tan^2\varphi_{\mathcal{F}}(t))^{1/2}\ y_{2t}} = \dfrac{z(t)}{(1+\tan^2\varphi_{\mathcal{F}}(t))^{1/2}\ y_{2t}} - x(t) + \dfrac{x(t)}{y_{2t}}v_2(t), \\ X_{\mathcal{S}}y_{3t} = x(t)y_{3t} - y(t) - (x(t) - X_{\mathcal{S}})\,v_3(t), \\ \dfrac{h}{(1+\tan^2\varphi_{\mathcal{S}}(t))^{1/2}} - X_{\mathcal{S}}y_{4t} = \dfrac{z(t)}{(1+\tan^2\varphi_{\mathcal{S}}(t))^{1/2}} - x(t)y_{4t} + (x(t) - X_{\mathcal{S}})\,v_4(t). \end{cases} \tag{16}$$

Finally, the precise values of $\tan\varphi_{\mathcal{F}}(t)$ and $\tan\varphi_{\mathcal{S}}(t)$ in (16) are unknown and have to be replaced by the corresponding observations y_{1t} and y_{3t}. As a result, from (16) we arrive at the approximate relations

$$\begin{cases} \dfrac{Y_{\mathcal{F}}}{y_{1t}} = \dfrac{y(t)}{y_{1t}} - x(t) + \dfrac{x(t)}{y_{1t}} v_1(t), \\ \dfrac{h}{\left(1+(y_{1t})^2\right)^{1/2}\ y_{2t}} = \dfrac{z(t)}{\left(1+(y_{1t})^2\right)^{1/2}\ y_{2t}} - x(t) + \dfrac{x(t)}{y_{2t}} v_2(t), \\ X_{\mathcal{S}} y_{3t} = x(t) y_{3t} - y(t) - (x(t) - X_{\mathcal{S}})\, v_3(t), \\ \dfrac{h}{\left(1+(y_{3t})^2\right)^{1/2}} - X_{\mathcal{S}} y_{4t} = \dfrac{z(t)}{\left(1+(y_{3t})^2\right)^{1/2}} - x(t) y_{4t} + (x(t) - X_{\mathcal{S}})\, v_4(t). \end{cases} \tag{17}$$

Following the method of pseudomeasurements, system (17) is used to write the filter; in particular, the left-hand sides are used as new observations. The reason is that the right-hand sides contain linear combinations of the estimated position $x(t)$, $y(t)$, and $z(t)$, which gives hope for a good performance of suboptimal Kalman filters, first of all, the extended Kalman filter (EKF) [8]. Indeed, this property is very attractive: when writing the EKF, there is no need to calculate the derivatives of the measuring functions (ψ_t in model (1)).

For the designed CMNF, this approach provides the basic correction in the form of the observation residual (17), i.e., $\zeta_t \in \mathbb{R}^4$ given by

$$\begin{cases} \zeta_{1t} = \dfrac{Y_{\mathcal{F}}}{Y_1} - \dfrac{X_2}{Y_1} + X_1, \quad \zeta_{2t} = \dfrac{h - X_3}{\left(1+(Y_1)^2\right)^{1/2}\ Y_2} + X_1, \\ (X_1, X_2, X_3)' = \widetilde{x}_{t-\widehat{\tau}_{\mathcal{F}}(t)}, \\ \zeta_{3t} = X_{\mathcal{S}} Y_3 - X_1 Y_3 + X_2, \quad \zeta_{4t} = \dfrac{h - X_3}{\left(1+(Y_3)^2\right)^{1/2}} - X_{\mathcal{S}} Y_4 + X_1 Y_4, \\ (X_1, X_2, X_3)' = \widetilde{x}_{t-\widehat{\tau}_{\mathcal{S}}(t)}. \end{cases} \tag{18}$$

In contrast to the correction term of the conventional EKF, the ultimate formula for ζ_t (18) incorporates, as the correction (15) of the typical CMNF, the observation delays with the same estimates $\widehat{\tau}_{\mathcal{F}}(t)$ and $\widehat{\tau}_{\mathcal{S}}(t)$.

Finally, the third structure for the CMNF is determined from geometric considerations, and the corresponding correction is called *geometric*. Again we use (10) under the assumption of no measurement errors. These relations can be interpreted as four joint equations for determining the three AUV coordinates $X,\ Y, Z$. Although the geometric problem in Fig. 1 has one solution (the surely intersecting acoustic ray lines of two beacons), system (10) can be formally solved in four ways. By combining the quantities measured by both beacons into the vector $(Y_1, Y_2, Y_3, Y_4)' = (\tan\varphi_{\mathcal{F}},\ \tan\lambda_{\mathcal{F}}, \tan\varphi_{\mathcal{S}}, \tan\lambda_{\mathcal{S}})'$, from (10) we obtain the system

$$\begin{cases} Y_1 = \dfrac{Y - Y_{\mathcal{F}}}{X}, \quad Y_2 = \dfrac{Z-h}{X} \dfrac{1}{\left(1+(Y_1)^2\right)^{1/2}}, \\ Y_3 = \dfrac{Y}{X - X_{\mathcal{S}}}, \quad Y_4 = \dfrac{Z-h}{X - X_{\mathcal{S}}} \dfrac{1}{\left(1+(Y_3)^2\right)^{1/2}}. \end{cases}$$

Its solution X, Y, Z satisfies each of the following twelve equalities:

$$\begin{cases} X = \dfrac{Y_{\mathcal{F}} + Y_3 X_{\mathcal{S}}}{Y_3 - Y_1}, \\ Y = \dfrac{Y_3\,(Y_{\mathcal{F}} + Y_1 X_{\mathcal{S}})}{Y_3 - Y_1}, \\ Z = h + Y_2 \dfrac{Y_{\mathcal{F}} + Y_3 X_{\mathcal{S}}}{Y_3 - y_1}\left(1 + (Y_1)^2\right)^{1/2}, \end{cases} \qquad \begin{cases} X = \dfrac{Y_{\mathcal{F}} + Y_3 X_{\mathcal{S}}}{Y_3 - Y_1}, \\ Y = \dfrac{Y_3\,(Y_{\mathcal{F}} + Y_1 X_{\mathcal{S}})}{Y_3 - Y_1}, \\ Z = h + Y_4\left(\dfrac{Y_{\mathcal{F}} + Y_3 X_{\mathcal{S}}}{Y_3 - Y_1} - X_{\mathcal{S}}\right)\left(1 + (Y_3)^2\right)^{1/2}, \end{cases}$$

$$\begin{cases} X = \dfrac{Y_4 X_{\mathcal{S}}}{Y_4 - Y_2\left(\frac{1+(Y_1)^2}{1+(Y_3)^2}\right)^{1/2}}, \\ Y = \dfrac{Y_1 Y_4 X_{\mathcal{S}}}{Y_4 - Y_2\left(\frac{1+(Y_1)^2}{1+(Y_3)^2}\right)^{1/2}} + Y_{\mathcal{F}}, \\ Z = h + \dfrac{Y_2 Y_4 X_{\mathcal{S}}}{\frac{Y_4}{\left(1+(Y_1)^2\right)^{1/2}} - \frac{Y_2}{\left(1+(Y_3)^2\right)^{1/2}}}, \end{cases} \qquad \begin{cases} X = \dfrac{Y_4 X_{\mathcal{S}}}{Y_4 - Y_2\left(\frac{1+(Y_1)^2}{1+(Y_3)^2}\right)^{1/2}}, \\ Y = \dfrac{Y_2 Y_3 X_{\mathcal{S}}}{Y_4\left(\frac{1+(Y_3)^2}{1+(Y_1)^2}\right)^{1/2} - Y_2}, \\ Z = h + \dfrac{Y_2 Y_4 X_{\mathcal{S}}}{\frac{Y_4}{\left(1+(Y_1)^2\right)^{1/2}} - \frac{Y_2}{\left(1+(Y_3)^2\right)^{1/2}}}. \end{cases}$$

Excluding the identical ones, we arrive at eight equalities based on the four measurements Y_1, Y_2, Y_3, Y_4. They can be used as the basic CMNF correction $\zeta_t \in \mathbb{R}^8$ of the form

$$\begin{cases} \zeta_{1t} = X_1 - \dfrac{Y_{\mathcal{F}} + Y_3 X_{\mathcal{S}}}{Y_3 - Y_1}, \;\; \zeta_{3t} = X_3 - h - Y_2 \dfrac{Y_{\mathcal{F}} + Y_3 X_{\mathcal{S}}}{Y_3 - Y_1}\left(1 + (Y_1)^2\right)^{1/2}, \\ \zeta_{2t} = X_2 - \dfrac{Y_3\,(Y_{\mathcal{F}} + Y_1 X_{\mathcal{S}})}{Y_3 - Y_1}, \;\; \zeta_{4t} = X_3 - h - Y_4\left(\dfrac{Y_{\mathcal{F}} + Y_3 X_{\mathcal{S}}}{Y_3 - Y_1} - X_{\mathcal{S}}\right)\left(1 + (Y_3)^2\right)^{1/2}, \\ \zeta_{5t} = X_1 - \dfrac{Y_4 X_{\mathcal{S}}}{Y_4 - Y_2\left(\frac{1+(Y_1)^2}{1+(Y_3)^2}\right)^{1/2}}, \;\; \zeta_{7t} = X_2 - \dfrac{Y_2 Y_3 X_{\mathcal{S}}}{Y_4\left(\frac{1+(Y_3)^2}{1+(Y_1)^2}\right)^{1/2} - Y_2}, \\ \zeta_{6t} = X_2 - \dfrac{Y_1 Y_4 X_{\mathcal{S}}}{Y_4 - Y_2\left(\frac{1+(Y_1)^2}{1+(Y_3)^2}\right)^{1/2}} - Y_{\mathcal{F}}, \;\; \zeta_{8t} = X_3 - h - \dfrac{Y_2 Y_4 X_{\mathcal{S}}}{\frac{Y_4}{\left(1+(Y_1)^2\right)^{1/2}} - \frac{Y_2}{\left(1+(Y_3)^2\right)^{1/2}}}, \\ (X_1, X_2, X_3)' = \widetilde{x}_{t-\max\left(\widehat{\tau}_{\mathcal{F}}(t), \widehat{\tau}_{\mathcal{S}}(t)\right)}, \;\; Y_{1(2)} = y_{1(2)t-\max\left(\widehat{\tau}_{\mathcal{F}}(t),\, \widehat{\tau}_{\mathcal{S}}(t)\right)+\widehat{\tau}_{\mathcal{F}}(t)}, \\ Y_{3(4)} = y_{3(4)t-\max\left(\widehat{\tau}_{\mathcal{F}}(t),\, \widehat{\tau}_{\mathcal{S}}(t)\right)+\widehat{\tau}_{\mathcal{S}}(t)}. \end{cases} \tag{19}$$

Here, the time delay estimates $\widehat{\tau}_{\mathcal{F}}(t)$ and $\widehat{\tau}_{\mathcal{S}}(t)$ are calculated by analogy with the two previous variants of correction but used in a slightly more complicated way. Since the geometric interpretation "mixes" measurements from different beacons, the delays are mixed as well; therefore, both the prediction and the measurements must be shifted back for referring to the same time instant. For the prediction, this is the shift by the larger of the values $\widehat{\tau}_{\mathcal{F}}(t)$ or $\widehat{\tau}_{\mathcal{S}}(t)$; for the observations, the shift by the difference $|\widehat{\tau}_{\mathcal{F}}(t) - \widehat{\tau}_{\mathcal{S}}(t)|$ toward the earlier measurement. (Recall that the measurements y_{it} in (19) have been already shifted by $\tau_{\mathcal{F}}(t)$ or $\tau_{\mathcal{S}}(t)$ according to model (13).) Thus, the current (most "fresh") observations will be used only halfway. This "damage" is in the interest of synchronizing the measurements. In fact, of course, we introduce no damage at all: the unused part of the observations will be employed very quickly after the desynchronization time $|\tau_{\mathcal{F}}(t) - \tau_{\mathcal{S}}(t)|$.

In the case of more beacons (three, four, etc. acoustic sensors), the number of equations (19) grows exponentially. So formally scaling the geometric correction to a larger number of observers may lead to an unacceptable computing cost due to the implementation complexity instead of

potentially improving the positioning quality. However, we hypothesize that there is no need to use all possible combinations of measurements, being limited to only some of them. In this case, it will be reasonable to employ all available sensors, no matter which pairs are involved in the correction. The success of the pseudomeasurement filter demonstrated in the next section indirectly confirms this hypothesis. Nevertheless, despite the simplicity of the geometric problem, the geometric variant of the correction procedure yields the best CMNF structure for solving the AUV positioning problem.

5. NUMERICAL EXPERIMENTS

To design the CMNF by the Monte Carlo method and analyze its quality, we simulated two independent samples of $N = 10\,000$ trajectories. On the first sample, the filter parameters (6) and (7) were calculated for each of the three correction structures proposed. Note that although relations (7) are not directly required to compute the filtering estimate, the values of $\widehat{K}_t$ are useful to know because they express the theoretical accuracy of the filter. On the second sample, we analyzed the real quality of the filtering estimate $\widehat{x}_t = (\widehat{x}(t), \widehat{y}(t), \widehat{z}(t))'$ and the identification estimate $\widehat{\mu}_t = (\widehat{v}_x(t), \widehat{v}_y(t), \widehat{v}_z(t))'$. The estimation accuracy was determined by the mean square deviations of the estimation errors, denoted by $\sigma_{\widehat{x}}(t)$, $\sigma_{\widehat{y}}(t)$, $\sigma_{\widehat{z}}(t)$ (indicated in meters in the figures) and $\sigma_{\widehat{v}_x}(t)$, $\sigma_{\widehat{v}_y}(t)$, $\sigma_{\widehat{v}_z}(t)$ (km/h) and calculated by the Monte Carlo method on the second sample. Thus, it is necessary to examine both the absolute values of these quantities (in particular, compare them with those calculated in the model without the time delays) and the difference between them

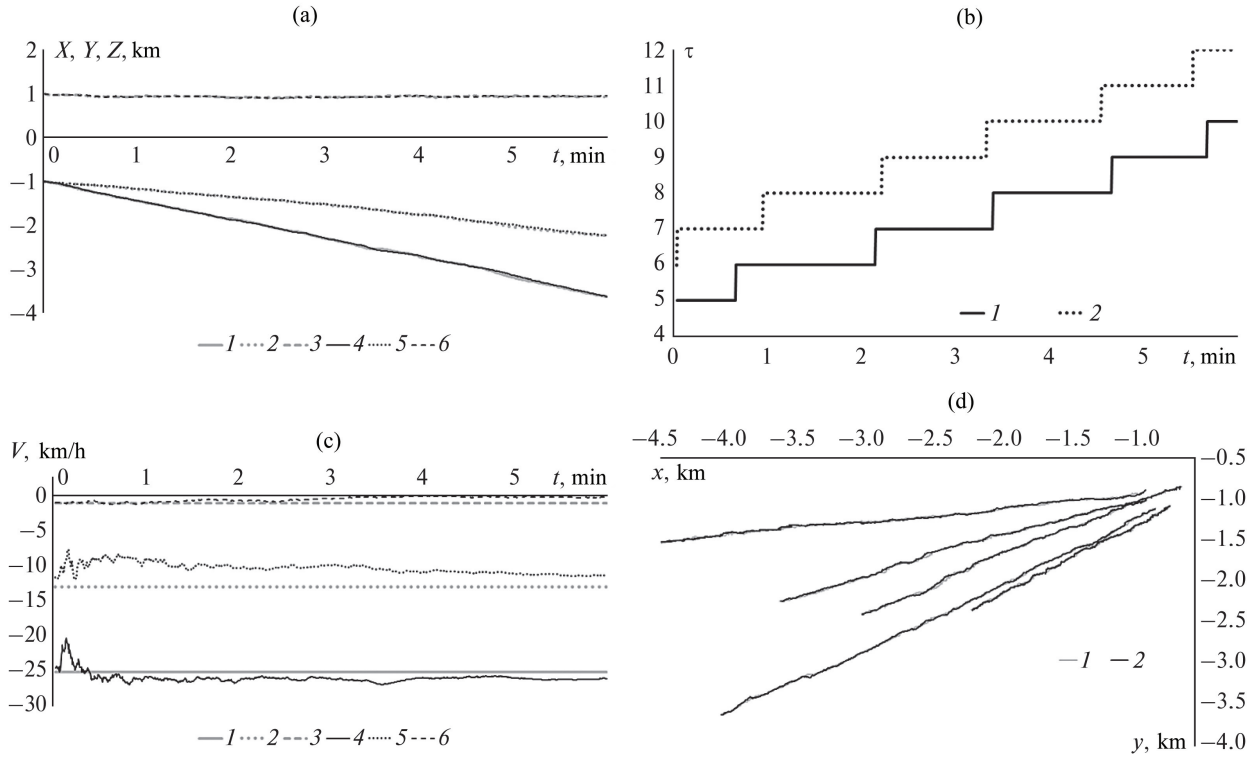

Fig. 3. AUV trajectories: (a) curves *1–3* correspond to the positions $x(t)$, $y(t)$, and $z(t)$, whereas curves *4–6* to the estimates $\widehat{x}(t)$, $\widehat{y}(t)$, and $\widehat{z}(t)$; (b) curves *1* and *2* correspond to the time delays $\tau_{\mathcal{F}}(t)$ and $\tau_{\mathcal{S}}(t)$; (c) curves *1–3* correspond to the velocities v_x, v_y, and v_z, whereas curves *4–6* to the estimates $\widehat{v}_x(t)$, $\widehat{v}_y(t)$, and $\widehat{v}_z(t)$; (d) curve *1* correspond to the AUV positions $(x(t), y(t))$, whereas curve *2* to the estimates $(\widehat{x}(t), \widehat{y}(t))$ on the trajectories.

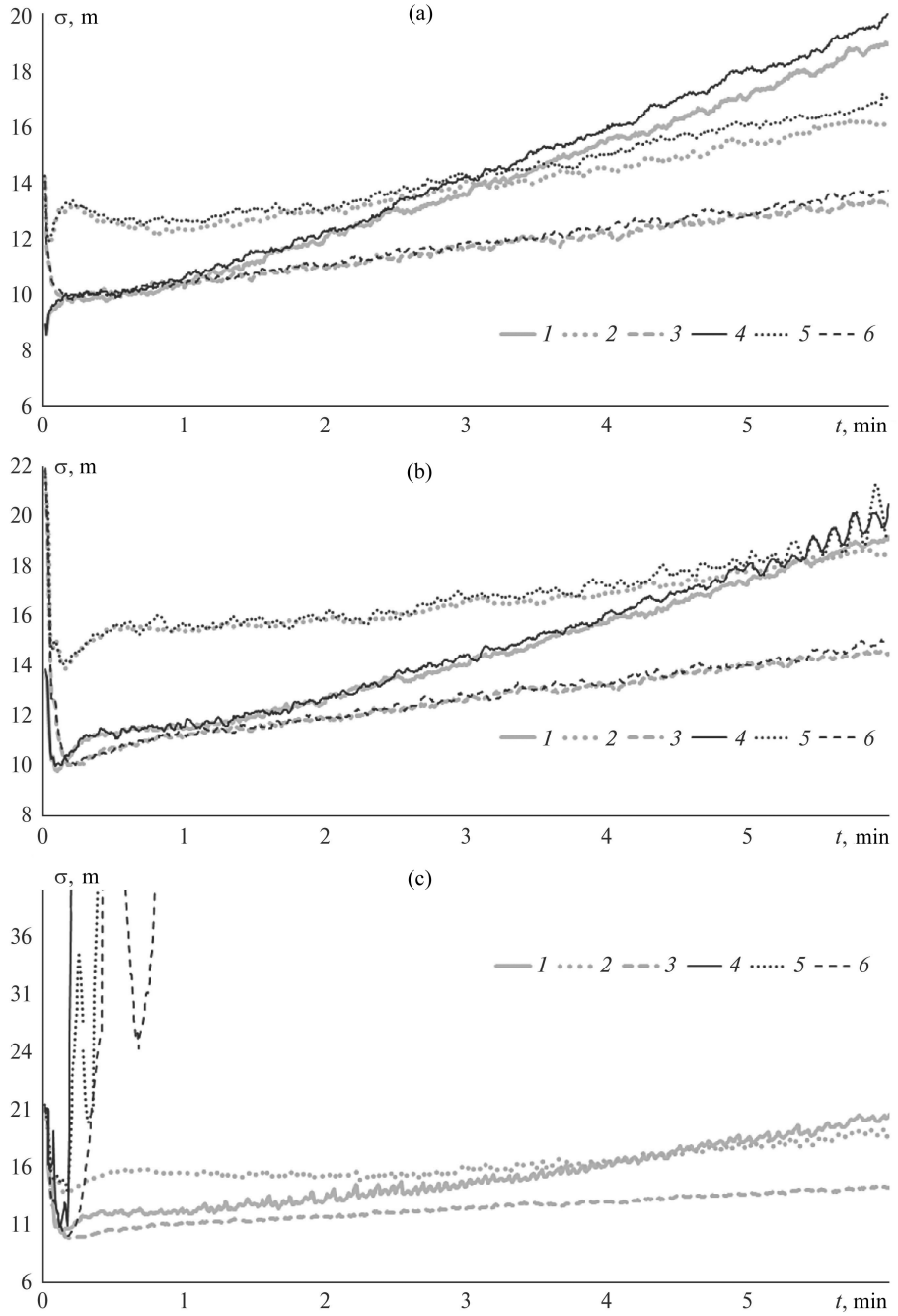

Fig. 4. Mean square deviations of the filters: (a) geometrical, (b) pseudomeasurements, and (c) typical. Curves *1–6* correspond to $\left(\widehat{K}_t\right)_{11}^{1/2}$, $\left(\widehat{K}_t\right)_{22}^{1/2}$, $\left(\widehat{K}_t\right)_{33}^{1/2}$, $\sigma_{\widehat{x}}(t)$, $\sigma_{\widehat{y}}(t)$, and $\sigma_{\widehat{z}}(t)$.

and the corresponding diagonal elements of $\widehat{K_t}$ in order to assess the practical realization of the theoretical properties of the CMNF in the case of its computer simulations-based design.

In Fig. 3, the experiment is illustrated with examples of characteristic position trajectories, time delay, filtering estimates, and parameter identification estimates. In Fig. 3a, one graph shows the coordinates of one AUV trajectory $x(t), y(t), z(t)$ and the corresponding CMNF estimate $\widehat{x}(t), \widehat{y}(t), \widehat{z}(t)$; in Fig. 3b, the time delays $\tau_{\mathcal{F}}(t)$ and $\tau_{\mathcal{S}}(t)$ for the first and second beacons on the same AUV trajectory; in Fig. 3c, the estimates $\widehat{v}_x(t), \widehat{v}_y(t), \widehat{v}_z(t)$ and the exact values of

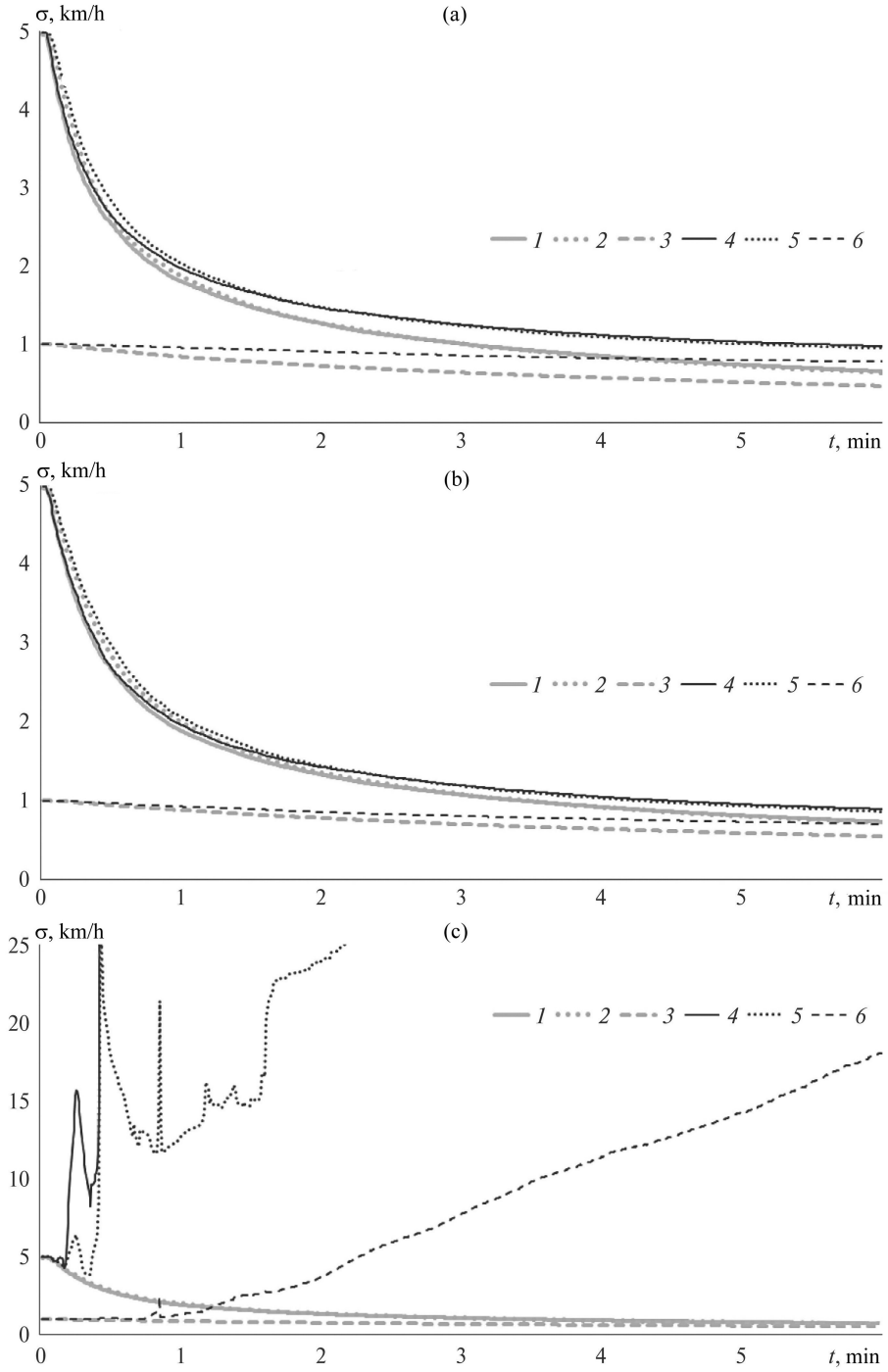

Fig. 5. Mean square deviations of the filters: (a) geometrical, (b) pseudomeasurements, and (c) typical. Curves *1–6* correspond to $\left(\widehat{K}_t\right)^{1/2}_{44}$, $\left(\widehat{K}_t\right)^{1/2}_{55}$, $\left(\widehat{K}_t\right)^{1/2}_{66}$, $\sigma_{\widehat{v}_x}(t)$, $\sigma_{\widehat{v}_y}(t)$, and $\sigma_{\widehat{v}_z}(t)$.

the velocities v_x, v_y, v_z; in Fig. 3d, several AUV trajectories in projection onto the Oxy plane. The CMNF estimates correspond to the geometric structure function. Although there exists a distinction in the filtering and identification estimates for different CMNF structures, it seems impossible to visualize this distinction on graphs. Therefore, numerical data are presented below to analyze the performance in detail.

Comparison of the estimation quality

Filter	$\sigma^{(1)}_{\widehat{x}}/\sigma^{(2)}_{\widehat{x}}$	$\sigma^{(1)}_{\widehat{y}}/\sigma^{(2)}_{\widehat{y}}$	$\sigma^{(1)}_{\widehat{z}}/\sigma^{(2)}_{\widehat{z}}$	$\sigma^{(1)}_{\widehat{v}_x}/\sigma^{(2)}_{\widehat{v}_x}$	$\sigma^{(1)}_{\widehat{v}_y}/\sigma^{(2)}_{\widehat{v}_y}$	$\sigma^{(1)}_{\widehat{v}_z}/\sigma^{(2)}_{\widehat{z}_x}$
$T = 15$, delay 54 s, unknown v_x, v_y, and v_z						
Geometric	13.80/**14.22**	13.93/**14.32**	11.61/**11.77**	**0.68**/0.99	**0.67**/0.97	**0.49**/0.79
Pseudomeasurements	14.36/14.60	16.54/16.83	12.60/12.70	0.76/**0.91**	0.75/**0.89**	0.56/**0.72**
Typical	15.22/**4300**	16.38/**3368**	12.50/**1117**	0.76/**88**	0.75/**96**	0.57/**17**
$T = 0$, delay 0 s, unknown v_x, v_y, and v_z						
Geometric	11.27/11.62	11.45/11.78	8.81/8.92	0.67/1.00	0.66/0.98	0.48/0.80
Pseudomeasurements	11.19/11.36	11.49/11.65	8.87/8.93	0.75/0.92	0.73/0.89	0.55/0.72
Typical	**11.09/11.25**	**11.45/11.61**	**8.81/8.86**	**0.74/0.92**	**0.73/0.89**	**0.55/0.72**
$T = 15$, delay 54 s, unknown $v_x = \mathrm{E}\{v_x\}$, $v_y = \mathrm{E}\{v_y\}$, and $v_z = \mathrm{E}\{v_z\}$						
Geometric	13.05/13.23	13.38/13.54	11.48/11.56	—	—	—
Pseudomeasurements	13.56/13.64	15.38/15.49	12.37/12.42	—	—	—
Typical	13.66/**45.81**	15.39/**32.22**	12.33/**22.09**	—	—	—
$T = 0$, delay 0 s, known $v_x = \mathrm{E}\{v_x\}$, $v_y = \mathrm{E}\{v_y\}$, and $v_z = \mathrm{E}\{v_z\}$						
Geometric	10.66/11.25	11.11/11.25	8.71/8.77	—	—	—
Pseudomeasurements	10.66/10.74	11.14/11.22	8.74/8.77	—	—	—
Typical	**10.65/10.72**	**11.13/11.21**	**8.71/8.75**	—	—	—

The next issue—the estimation accuracy—is illustrated in Figs. 4 and 5. Figures 4a–4c show the deviations $\sigma_{\widehat{x}}(t), \sigma_{\widehat{y}}(t), \sigma_{\widehat{y}}(t)$, and $\sigma_{\widehat{z}}(t)$ and, for comparison, the corresponding diagonal elements of the theoretical covariance $\widehat{K}_t$ of the estimation error. Figures 5a–5c present the similar characteristics $\sigma_{\widehat{v}_x}(t), \sigma_{\widehat{v}_y}(t)$, and $\sigma_{\widehat{v}_z}(t)$ for the identified velocities. Each figure contains three graphs corresponding to the three variants of the CMNF (geometric, pseudomeasurements, and typical).

Assessing these graphs visually, we state that the first two CMNF variants are successful in the positioning task. A precise comparison requires numerical indicators, which are given below. Also, the graphs confirm the fundamental possibility of velocity identification by these filters. The values characterizing the quality of identification are presented below. Obviously, the typical filter is able neither to position the AUV nor to identify the average velocity of motion. The discrepancy between the theoretical accuracy determined by the matrix $\widehat{K}_t$ and the real values of the deviations $\sigma_{\widehat{x}}(t), \sigma_{\widehat{y}}(t), \sigma_{\widehat{z}}(t)$, $\sigma_{\widehat{v}_x}(t), \sigma_{\widehat{v}_y}(t)$, and $\sigma_{\widehat{v}_z}(t)$ calculated on the second sample is too large. The reason consists in an insufficient sample size used for filter design and can be eliminated by significantly increasing N. However, in this case, the calculations become rather resource-intensive. It would make sense to consume computational resources only without the advantages of the other two CMNF structures, which are slightly more difficult to implement but much more efficient.

To conclude the experiment, it is necessary to characterize the real difference of the successful CMNF structures, the effect of the model with time delay on the quality of estimation, and the presence of identifiable parameters. For this purpose, we carried out calculations with the models in which $\tau_{\mathcal{F}}(t) = \tau_{\mathcal{S}}(t) = 0$, and the models in which $v_x = \mathrm{E}\{v_x\}$, $v_y = \mathrm{E}\{v_y\}$, $v_z = \mathrm{E}\{v_z\}$. The choice of the model without the time delay for comparison is clear; however, the assumption of a known constant velocity of the AUV on each trajectory may seem redundant. In fact, if the velocities are determined for each trajectory, as the original motion model (8) assumes, there will be no significant difference between positioning with the velocities known at the initial time

instant and positioning with the velocities given by the identification estimates. This is explained in Figs. 5a and 5b, showing that the filter produces an acceptable estimate of the current velocity rather quickly. In addition, the motion model (8) yields a fairly accurate prediction using the average velocity as well; under the assumption of no time delays, the velocity does not affect the positioning quality at all, although there is the possibility to identify it.

The time-averaged mean deviations were used as an objective measure of the positioning quality (averaging over 1000 steps, 6 min). For example, for the analysis of $\widehat{x}(t)$, $\sigma^{(2)}_{\widehat{x}} = \frac{1}{1000}\sum_{t=1}^{1000}\sigma_{\widehat{x}}(t)$ were calculated to compare $\sigma_{\widehat{x}}(t)$ with the theoretical accuracy $\sigma^{(1)}_{\widehat{x}} = \frac{1}{1000}\sum_{t=1}^{1000}\left(\widehat{K}_t\right)^{1/2}_{11}$. The values of $\sigma^{(1)}_{\widehat{v}_x} = \frac{1}{100}\sum_{t=901}^{1000}\left(\widehat{K}_t\right)^{1/2}_{44}$ and $\sigma^{(2)}_{\widehat{v}_x} = \frac{1}{100}\sum_{t=901}^{1000}\sigma_{\widehat{v}_x}(t)$, etc. (the mean deviations of the estimates at the last hundred steps) were determined to analyze the identification results. Here, the superscripts (1) and (2) indicate the deviation computed on the first (the theoretical accuracy) and second (the factual accuracy) sample, respectively, and the subscript denotes the estimate. All results are combined in the table; the most interesting ones, illustrating the highest and lowest precision estimates, are set off in bold.

6. CONCLUSIONS

Of course, supplementing the model with random time delays [5, 6] with the unknown parameters to be identified has complicated the technical implementation of estimation algorithms. Even a reliable approach involving the concepts of conditionally optimal and conditionally minimax filtering suffers from certain difficulties. This is the first important conclusion from the results presented in the table above. Reproducing the Kalman filter structure, the typical filter essentially turns out to be unworkable. Interestingly, in the models without delays, both the filter based on the residual and the filters of more complex structure cope equally well with positioning (estimation of the position coordinates) and identification (estimation of the velocity). Actually, in the case of no time delays in observations, the CMNF works equally with any structure and provides very good estimation accuracy.

The second remark should be made regarding the concept of pseudomeasurements [15]. The fact that this approach would give a workable CMNF structure in the model with delays did not initially seem obvious. Its ability to compete with a purely geometric solution was all the more questionable. As the result of this study, we have obtained quite competitive estimates in terms of accuracy; in the identification problem, the CMNF with the pseudomeasurement structure even outperforms the geometric filter. Moreover, the geometric solution cannot be obtained in several cases, and increasing the number of observers will lead to an exponential growth of the dimensions. At the same time, the concept of linear pseudomeasurements has a universal character, applies to any DOA sensors, and is much easier to implement.

Finally, the third remark concerns the interpretation of the identification results. On the one hand, using the Monte Carlo method, one cannot expect the convergence of estimates in a numerical experiment. On the other hand, the Bayesian approach to parameter estimation and the CMNF properties do not imply convergence in a finite time, only ensuring that the estimation quality will improve from step to step. The real deviation of the velocity estimate turns out to be about 1 km/h; for the coordinates x and y with the initial velocity of 5 km/h and 6 min observations, this result seems to be good. The velocity along the Oz axis is poorly estimated, but it has a much smaller effect on positioning accuracy. Thus, the fundamental possibility of identifying the velocities without direct measurements, such as Doppler sensors, has been confirmed by the experiment. Velocity measurements can further improve the accuracy of both motion model identification and AUV positioning.

ACKNOWLEDGMENTS

This work was performed using the infrastructure of the Shared Research Facilities "High Performance Computing and Big Data" (CKP "Informatics") of the Federal Research Center "Computer Science and Control," Russian Academy of Sciences (Moscow).

REFERENCES

1. Bar-Shalom, Y., Li, X.-R., and Kirubarajan, T., *Estimation with Applications to Tracking and Navigation: Theory, Algorithms and Software*, John Wiley & Sons, 2002.
2. *Autonomous Underwater Vehicles: Design and Practice (Radar, Sonar & Navigation)*, Ehlers, F., Ed., London: SciTech Publishing, 2020.
3. Kebkal, K.G. and Mashoshin, A.I., AUV Acoustic Positioning Methods, *Gyroscopy Navig.*, 2017, vol. 8, pp. 80–89.
4. Christ, R.D. and Wernli, R.L., *The ROV Manual: A User Guide for Remotely Operated Vehicles*, 2nd ed., Oxford: Butterworth-Heinemann, 2013.
5. Bosov, A.V., Observation-Based Filtering of State of a Nonlinear Dynamical System with Random Delays, *Autom. Remote Control*, 2023, vol. 84, no. 6, pp. 671–684.
6. Bosov, A., Tracking a Maneuvering Object by Indirect Observations with Random Delays, *Drones*, 2023, vol. 7, no. 7, art. no. 468.
7. Bosov, A.V., Nonlinear Dynamic System State Optimal Filtering by Observations with Random Delays, *Informatics and Applications*, 2023, vol. 17, no. 3, pp. 8–17.
8. Bernstein, I. and Friedland, B., Estimation of the State of a Nonlinear Process in the Presence of Nongaussian Noise and Disturbances, *J. Franklin Instit.*, 1966, vol. 281, no. 6, pp. 455–480.
9. Arulampalam, S., Maskell, S., Gordon, N.J., and Clapp, T., A Tutorial on Particle Filters for Online Non-linear/Non-Gaussian Bayesian Tracking, *IEEE Trans. Signal Processing*, 2002, vol. 50, no. 2, pp. 174–188.
10. Julier, S.J., Uhlmann, J.K., and Durrant-Whyte, H.F., A New Approach for Filtering Nonlinear Systems, *Proc. IEEE Amer. Control Conf. (ACC'95)*, 1995, pp. 1628–1632.
11. Pugachev, V.S., Recursive Estimation of Variables and Parameters in Stochastic Systems Described by Difference Equations, *Dokl. Akad. Nauk SSSR*, 1978, vol. 243, no. 5, pp. 1131–1133.
12. Pugachev, V.S., Estimation of Variables and Parameters in Discrete-Time Nonlinear Systems, *Autom. Remote Control*, 1979, vol. 40, no. 4, pp. 39–50.
13. Pankov, A.R. and Bosov, A.V., Conditionally Minimax Algorithm for Nonlinear System State Estimation, *IEEE Trans. Autom. Control*, 1994, vol. 39, no. 8, pp. 1617–1620.
14. Pugachev, V.S. and Sinitsyn, I.N., *Stochastic Differential Systems–Analysis and Filtering*, Chichester: Wiley, 1987.
15. Lin, X., Kirubarajan, T., Bar-Shalom, Y., and Maskell, S., Comparison of EKF, Pseudomeasurement, and Particle Filters for a Bearing-Only Target Tracking Problem, in *SPIE Proceedings. Signal and Data Processing of Small Targets 2002 (AEROSENSE 2002)*, Drummond, O.E., Ed., Orlando, April 1–5, 2002, SPIE: Bellingham, 2002, vol. 4728, pp. 240–250.
16. Miller, A. and Miller, B., Stochastic Control of Light UAV at Landing with the Aid of Bearing-Only Observations, in *SPIE Proceedings. Eight International Conference on Machine Vision (ICMV-2015)*, Verikas, A., Radeva, P., and Nikolaev, D., Eds., Barcelona, November 19–21, 2015, SPIE: Bellingham, 2015, vol. 9875, pp. 474–483.
17. Huber, P.J. and Ronchetti, E.M., *Robust Statistics*, 2nd. ed., Wiley, 2011.
18. Ljung, L., *System Identification—Theory for the User*, 2nd ed., NJ: PTR Prentice Hall, 1999.
19. Bertsekas, D.P. and Shreve, S.E., *Stochastic Optimal Control: The Discrete-Time Case*, NY: Academic Press, 1978.
20. Albert, A., *Regression and the Moor–Penrose Pseudoinverse*, New York: Academic Press, 1972.

21. Miller, A., Miller, B., and Miller, G., AUV Navigation with Seabed Acoustic Sensing, *Proceedings of the 2018 Australian New Zealand Control Conference (ANZCC)*, Melbourne, VIC, Australia, December 7–8, 2018, pp. 166–171.
22. Miller, A., Miller, B., and Miller, G., On AUV Control with the Aid of Position Estimation Algorithms Based on Acoustic Seabed Sensing and DOA Measurements, *Sensors*, 2019, vol. 19, art. no. 5520.
23. Miller, A., Miller, B., and Miller, G., Navigation of Underwater Drones and Integration of Acoustic Sensing with Onboard Inertial Navigation System, *Drones*, 2021, vol. 5, art. no. 83.
24. Hodges, R., *Underwater Acoustics: Analysis, Design and Performance of Sonar*, New York: Wiley, 2011.
25. Weirathmueller, M., Weber, T.C., Schmidt, V., McGillicuddy, G., Mayer, L., and Huff, L., Acoustic Positioning and Tracking in Portsmouth Harbor, New Hampshire, *Proc. OCEANS 2007*, Vancouver, BC, September 29– October 4, 2007, pp. 1–4.
26. Wong, G.S.K. and Zhu, S.-M., Speed of Sound in Seawater as a Function of Salinity, Temperature, and Pressure, *J. Acoust. Soc. Am.*, 1995, vol. 97, pp. 1732–1736.
27. Dushaw, B.D., Worcester, P.F., Cornuelle, B.D., and Howe, B.M., On Equations for the Speed of Sound in Seawater, *J. Acoust. Soc. Am.*, 1993, vol. 93, pp. 255–275.

This paper was recommended for publication by B.M. Miller, a member of the Editorial Board